FGF23 alleviates neuronal apoptosis and inflammation, and promotes locomotion recovery via activation of PI3K/AKT signalling in spinal cord injury

YAN CUI[1], BIN YANG[1], SHAOYI LIN[1], LUQIANG HUANG[1], FEIBIN XIE[1], WEI FENG[2] and ZHENZONG LIN[1]

Departments of [1]Orthopaedic Trauma and [2]Neurosurgery, Zhongshan Hospital Affiliated to Xiamen University, Xiamen, Fujian 361004, P.R. China

Received September 29, 2022; Accepted March 24, 2023

DOI: 10.3892/etm.2023.12039

Abstract. Fibroblast growth factor 23 (FGF23) regulates neuronal morphology, synaptic growth and inflammation; however, its involvement in spinal cord injury (SCI) remains unclear. Therefore, the present study aimed to investigate the effect of FGF23 on neuronal apoptosis, inflammation and locomotion recovery, as well as its underlying mechanism in experimental SCI models. Primary rat neurons were stimulated with H_2O_2 to establish an *in vitro* model of SCI and were then transfected with an FGF23 overexpression (oeFGF23) or short hairpin RNA (shFGF23) adenovirus-associated virus and treated with or without LY294002 (a PI3K/AKT inhibitor). Subsequently, an SCI rat model was constructed, followed by treatment with oeFGF23, LY294002 or a combination of the two. FGF23 overexpression (oeFGF23 vs. oeNC) decreased the cell apoptotic rate and cleaved-caspase3 expression, but increased Bcl-2 expression in H_2O_2-stimulated neurons, whereas shFGF23 transfection (shFGF23 vs. shNC) exhibited the opposite effect (all P<0.05). Furthermore, FGF23 overexpression (oeFGF23 vs. oeNC) could activate the PI3K/AKT signalling pathway, whereas treatment with the PI3K/AKT inhibitor (LY294002) (oeFGF23 + LY294002 vs. LY294002) attenuated these effects in H_2O_2-stimulated neurons (all P<0.05). In SCI model rats, FGF23 overexpression (oeFGF23 vs. oeNC) reduced the laceration and inflammatory cell infiltration in injured tissue, decreased TNF-α and IL-1β levels, and improved locomotion recovery (all P<0.05); these effects were attenuated by additional administration of LY294002 (oeFGF23 + LY294002 vs. LY294002) (all P<0.05). In conclusion, FGF23 alleviated neuronal apoptosis and inflammation, and promoted locomotion recovery via activation of the PI3K/AKT signalling pathway in SCI, indicating its potential as a treatment option for SCI; however, further studies are warranted for validation.

Correspondence to: Dr Zhenzong Lin, Department of Orthopaedic Trauma, Zhongshan Hospital Affiliated to Xiamen University, 201-209 South Hubin Road, Siming, Xiamen, Fujian 361004, P.R. China
E-mail: cuiyan@xmu.edu.cn

Dr Wei Feng, Department of Neurosurgery, Zhongshan Hospital Affiliated to Xiamen University, 201-209 South Hubin Road, Siming, Xiamen, Fujian 361004, P.R. China
E-mail: fengstat1@163.com

Key words: fibroblast growth factor 23, spinal cord injury, inflammation, apoptosis, PI3K/AKT signalling

Introduction

Spinal cord injury (SCI) is mainly induced by mechanical injuries, such as falls and traffic accidents, and is a public health issue with a global prevalence of 280-1,298 per 1,000,000 individuals (1,2). The pathophysiology of SCI is traditionally separated into two phases: Primary injury (the injury caused by the initial traumatic event) and secondary injury (delayed and progressive tissue injury, including the infiltration of inflammatory cells) (3,4). Regarding the primary injury, treatment mainly focuses on early acute care; for secondary injury, therapeutic approaches include traditional drug therapy, surgery, cell therapy, gene therapy and tissue engineering (5-7). However, considering the limited efficacy and unsatisfactory prognosis of the present treatment approaches, it would be valuable to further investigate the pathogenesis of SCI and develop more effective therapeutic targets.

The fibroblast growth factor (FGF) family comprises 18 secreted proteins that modulate neural development, metabolism and function via multiple signalling pathways (8,9). FGF23 is mainly secreted by the osteoblastic lineage and detected in the cerebrospinal fluid, it also exhibits a regulatory effect on neuronal properties (10-12). For example, previous studies have revealed that FGF23 has a fundamental role in mediating neuronal morphology, synaptic density, presympathetic neuronal activity and inflammatory cytokine secretion through several mechanisms, such as FGF receptor-Klotho complexes and the NF-κB signalling pathway (11-14); however, the role of FGF23 in SCI remains unclear. The current study aimed to investigate the effects of FGF23 on neural apoptosis, inflammation and locomotion recovery, as well as its underlying mechanism in SCI.

Materials and methods

Animals. Male Sprague Dawley (SD) rats (n=60; weight, 200±20 g; age, 4-6 weeks) were purchased from Jiangsu Laboratory Animal Centre and housed under standard conditions (12-h dark/light cycle; temperature, 23±2˚C; *ad libitum* access to food and water; relative humidity, 40-60%). All procedures were approved by the Animal Care and Use Committee of Xiamen University (approval no. 20210401; Xiamen, China). Morbidity was used as the humane endpoint in the present study. These endpoints were applied following the criteria delineated in the 'Guidelines for Endpoints in Animal Study Proposals' at the Zhongshan Hospital Affiliated to Xiamen University (15). The humane endpoints included: i) The animal exhibited symptoms including, but not limited to, a lack of responsiveness to manual stimulation, and/or immobility and an inability to eat or drink; ii) laboured breathing and cyanosis; iii) diarrhoea or urinary incontinence; iv) severe, rapid weight loss and emaciation (maximum 20% of body weight from baseline); v) impaired mobility; vi) other situations where a veterinarian had determined that euthanasia was necessary.

Primary neuron culture. Primary neurons were cultured as previously described (16). Briefly, a pregnant SD rat was anaesthetized by intraperitoneal injection of 50 mg/kg pentobarbital sodium and rapidly sacrificed using CO_2 inhalation (50% chamber volume/min). Subsequently, the cerebral cortex of the six embryos (embryonic day 16) was cut into ~1-mm pieces and isolated using trypsin (Sangon Biotech Co., Ltd.) for 20 min at 37˚C. After being centrifuged (300 x g; 5 min; room temperature), cells were resuspended and seeded into poly-D-lysin-coated plates (Corning, Inc.). Cells were then cultured in Neurobasal-A medium (Gibco; Thermo Fisher Scientific, Inc.) supplemented with B-27™ supplement (Gibco; Thermo Fisher Scientific, Inc.) and 100 U/ml penicillin/streptomycin (Sangon Biotech Co., Ltd.) at 37˚C with 5% CO_2. The medium was replaced every 2 days and primary neurons were harvested after 10 days of culture.

H_2O_2 stimulation. The primary neurons were plated into a 6-well plate ($5x10^5$ cells/well) and were divided into two groups: The H_2O_2 group, in which primary neurons were treated with 100 μM H_2O_2 (Beijing Solarbio Science & Technology Co., Ltd.) (17,18); the normal group, in which the primary neurons were cultured without H_2O_2 stimulation. After 24 h of stimulation at 37˚C, cells were harvested for reverse transcription-quantitative PCR (RT-qPCR), western blotting and apoptosis analysis.

FGF23 regulation. The FGF23 overexpression adeno-virus-associated virus (AAV; oeFGF23), short hairpin (sh)RNA AAV (shFGF23) and negative control (NCs) AAVs (oeNC and shNC) were purchased from Shanghai GenePharma Co., Ltd. Briefly, primary neurons were seeded into 6-well plates ($5x10^5$ cells/well) and infected (multiplicity of infection, 50) with overexpression NC AAV (oeNC), oeFGF23, shRNA NC AAV (shNC) or shFGF23 at 37˚C for 24 h. The sense sequences for shNC and shFGF23 were: 5'-GTTCTCCGAACGTGTCACGTTTCAAGAGAACGTGACACGTTCGGAGAAC-3' and 5'-GGAACAGCTATCACCTACATTCAAGAGATGTAGGTGATAGCTGTTCC-3', respectively. Uninfected primary neurons were used as control cells. After being cultured for 48 h at 37˚C, cells in all groups were stimulated with 100 μM H_2O_2 for 24 h at 37˚C and harvested for RT-qPCR, western blotting and apoptosis analysis.

LY294002 treatment. oeNC- or oeFGF23-infected cells were seeded into 6-well plates ($5x10^5$ cells/well) and divided into the following groups: OeNC, cells infected with oeNC; oeFGF23, cells infected with oeFGF23; LY294002, cells infected with oeNC and incubated with 10 μM LY294002 (PI3K inhibitor; MedChemExpress) at 37˚C for 12 h (19); and oeFGF23 + LY294002, cells infected with oeFGF23 and incubated with 10 μM LY294002 at 37˚C for 12 h. Primary neurons without infection or inhibitor treatment were used as the control group. The primary neurons in all groups were then stimulated with 100 μM H_2O_2 for 24 h at 37˚C. Finally, the cells were harvested for RT-qPCR, western blotting and apoptosis analysis.

RT-qPCR. RT-qPCR was performed to assess FGF23 mRNA expression levels in primary neurons. Briefly, total RNA was extracted from $1x10^6$ primary neurons using TRIzol® reagent (Invitrogen; Thermo Fisher Scientific, Inc.). Subsequently, RNA was reverse transcribed into cDNA using a PrimeScript™ RT reagent kit (Takara Bio, Inc.) according to manufacturer's protocols. qPCR amplification was performed using a TB Green® Fast qPCR mix kit (Takara Bio, Inc.), and relative mRNA expression levels of FGF23 were calculated using the $2^{-\Delta\Delta Cq}$ method (20). The primer sequences were as follows: FGF23 forward, 5'-TGGCCATGTAGACGGAACAC-3' and reverse, 5'-GGCCCCTATTATCACTACGGAG-3'; and GAPDH forward, 5'-CAAGTTCAACGGCACAGTCAAG-3' and reverse, 5'-ACATACTCAGCACCAGCATCAC-3'. The thermocycling conditions were as follows: 95˚C for 30 sec (one cycle), followed by 40 cycles at 95˚C for 5 sec and 61˚C for 20 sec.

Apoptosis assay. The apoptotic rate of primary neurons was detected using an Annexin V-FITC/PI Cell Apoptosis Detection Kit (Beyotime Institute of Biotechnology). Briefly, infected or treated cells were washed twice with precooled PBS and adjusted to $2x10^6$ cells/ml. Subsequently, 5 μl Annexin V-FITC and 5 μl PI were added to the cell suspension for 10 min at room temperature. Flow cytometric analysis was carried out using the FACSCanto II flow cytometer (BD Biosciences). The data were analysed using FlowJo 7.6.1 (BD Biosciences).

SCI model and treatment. The SCI rat model was constructed as previously described (21). The SD rats were anaesthetized by intraperitoneal injection of 50 mg/kg pentobarbital sodium and a laminectomy was performed at the T9 vertebral section to expose the spinal cord. Subsequently, the spinal cord was contused with a force of 200 kDyne using the Infinite Horizon Impactor (Precision Systems & Instrumentation). Injection of AAV or PBS at the site of injury was performed after the surgery. The rats were divided into five groups: Sham group (n=12), which received only laminectomy without contusion and 10 μl PBS injection;

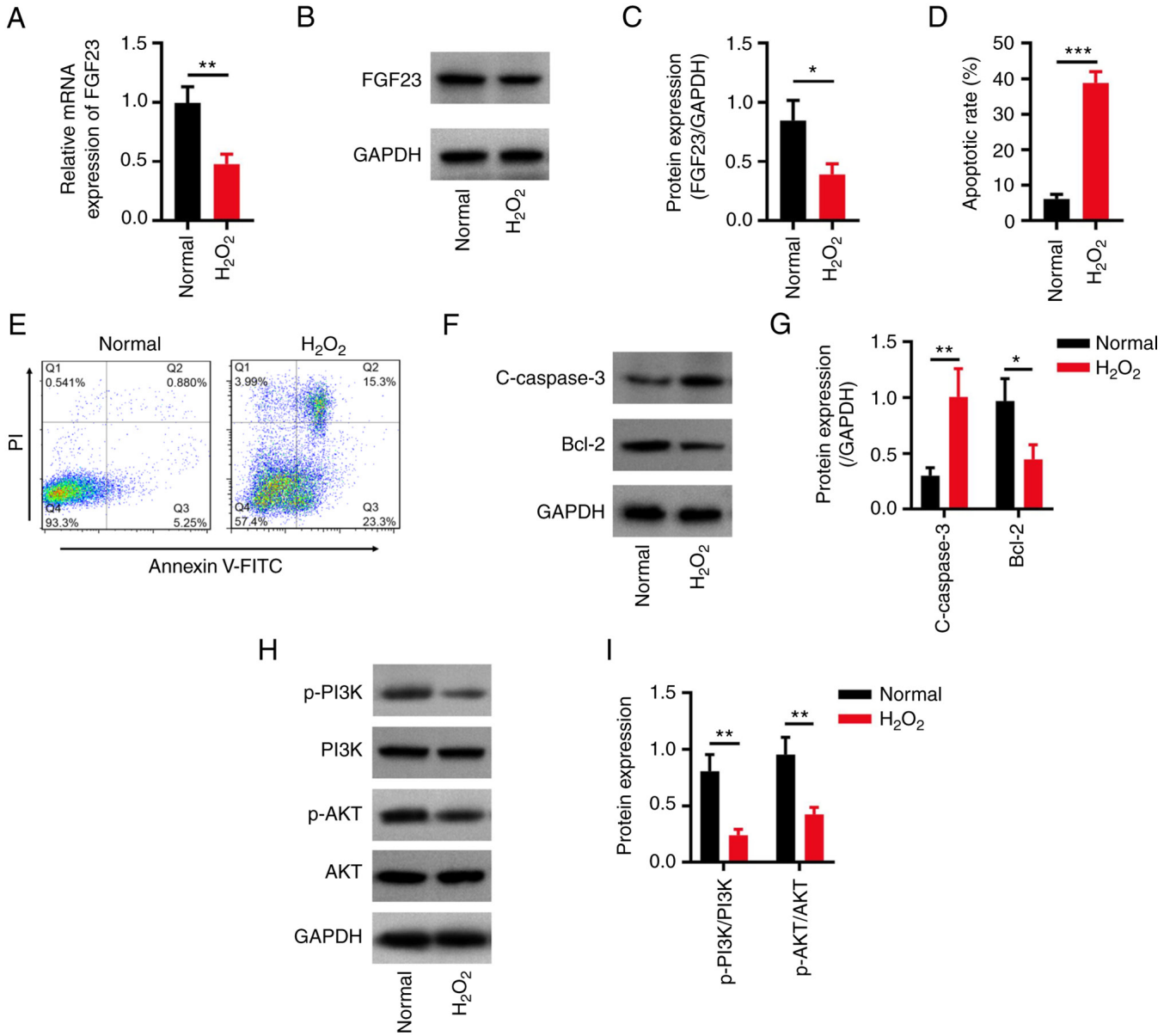

Figure 1. Cell apoptosis, FGF23 and PI3K/AKT signalling in H_2O_2-stimulated primary neurons. (A) Relative mRNA expression levels, (B) representative western blotting images of FGF23 and (C) FGF23/GAPDH level. (D) Semi-quantification of apoptotic rates and (E) representative flow cytometry plots of Annexin V/PI staining. (F) Representative western blotting images and (G) relative protein expression levels of C-caspase3 and Bcl-2. (H) Representative western blotting images and (I) relative expression ratios of p-PI3K/PI3K and p-AKT/AKT. GAPDH was used as a loading control. *P<0.05, **P<0.01 and ***P<0.001. C-, cleaved; FGF23, fibroblast growth factor 23; p-, phosphorylated.

SCI group (n=12), which received SCI surgery and 10 μl PBS injection; SCI + oeNC group (n=12), which received SCI surgery and 10 μl oeNC injection; SCI + oeFGF23 group (n=12), which received SCI surgery and 10 μl oeFGF23 injection; and SCI + oeFGF23 + LY294002 group (n=12), which received SCI surgery, 10 μl oeFGF23 injection and LY294002 injection (0.3 mg/kg/day; intravenous) (22). At 7 days post-operation, rats were anaesthetized by intraperitoneal injection of 50 mg/kg pentobarbital sodium and rapidly sacrificed using CO_2 asphyxiation (50% chamber volume/min) and spinal cord lesion tissues (n=6/group) were harvested for western blotting. In the remaining rats, Basso-Beattie-Bresnahan (BBB) scoring (23) was performed to assess the locomotion recovery at 1, 3, 7, 10, 14, 21 and 28 days after surgery (n=6/group). At 28 days post-surgery, the rats were anaesthetized by intraperitoneal injection of 50 mg/kg pentobarbital sodium and rapidly sacrificed using CO_2 asphyxiation (50% chamber volume/min), and spinal cord lesion tissues were collected for H&E and TUNEL staining, and ELISA. The death of the rats was confirmed following the AVMA Guidelines for the Euthanasia of Animals: 2020 Edition, including lack of pulse, breathing, corneal reflex and response to firm toe pinch; inability to hear respiratory sounds and heartbeat by use of a stethoscope; greying of the mucous membranes; and rigor mortis (24).

H&E and TUNEL staining. The spinal cord lesion tissues were fixed with 4% paraformaldehyde (Beyotime Institute of Biotechnology) for 24 h at room temperature, embedded in paraffin and cut into sections (4 μm). H&E staining was

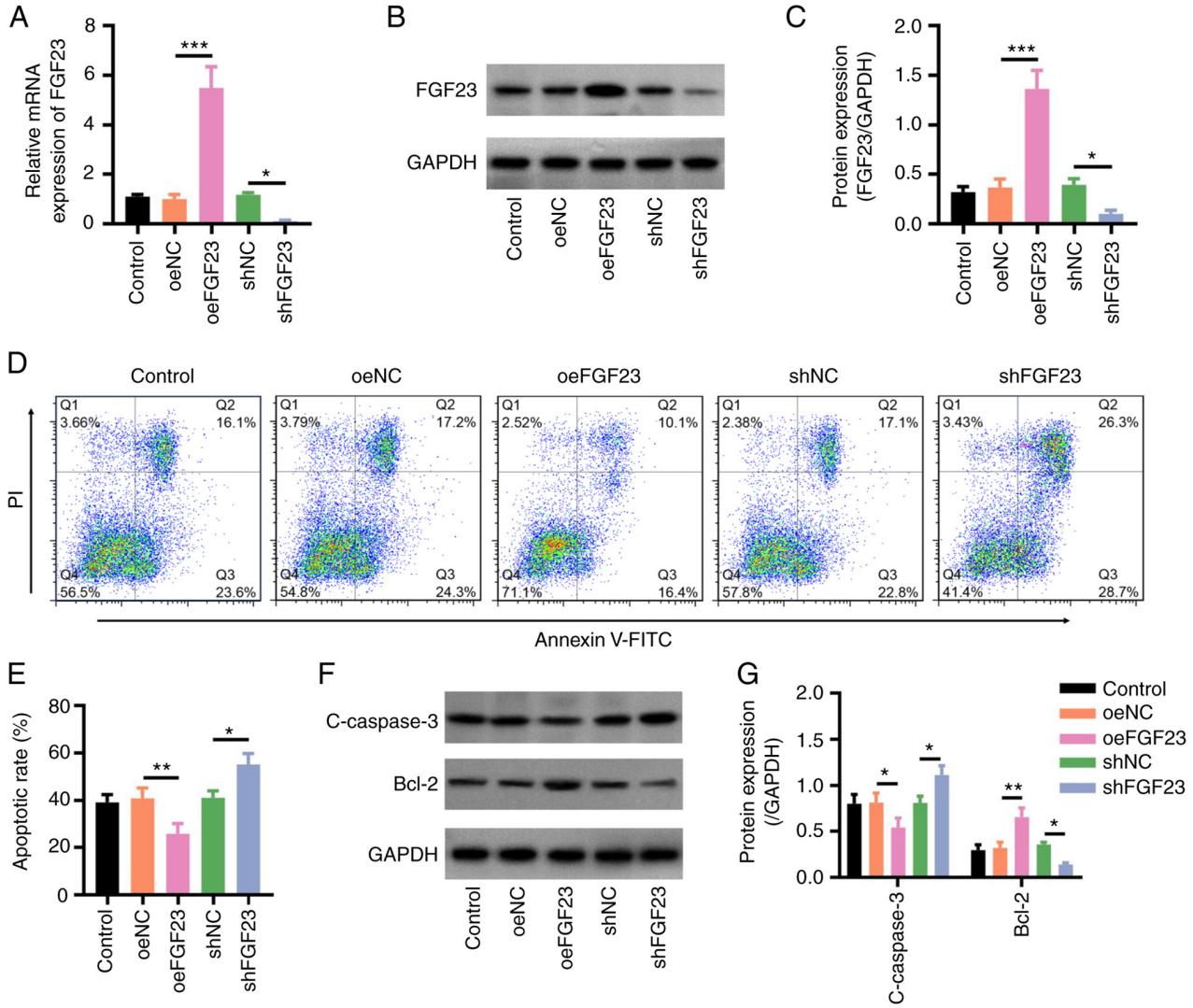

Figure 2. FGF23 overexpression inhibits H_2O_2-stimulated neuronal apoptosis. (A) Relative mRNA expression levels of FGF23 in the control, oeNC, oeFGF23, shNC and shFGF23 groups. (B) Representative western blotting images and (C) relative protein expression levels of FGF23. (D) Representative flow cytometry plots of Annexin V/PI staining, and (E) quantification of apoptotic rates. (F) Representative western blotting images and (G) relative protein expression levels of C-caspase3 and Bcl-2. *P<0.05, **P<0.01 and ***P<0.001. C-, cleaved; FGF23, fibroblast growth factor 23; NC, negative control; oe, overexpression; sh, short hairpin RNA.

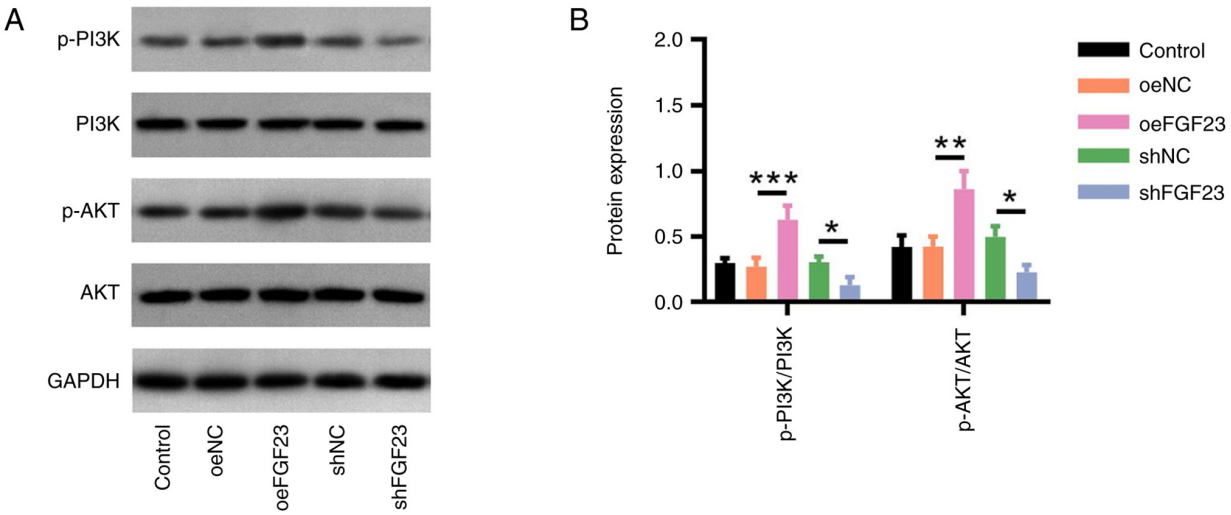

Figure 3. FGF23 activates PI3K/AKT signalling. (A) Representative western blotting images and (B) protein expression ratios of p-PI3K/PI3K and p-AKT/AKT in the control, oeNC, oeFGF23, shNC and shFGF23 groups. *P<0.05, **P<0.01 and ***P<0.001. FGF23, fibroblast growth factor 23; NC, negative control; oe, overexpression; p-, phosphorylated; sh, short hairpin RNA.

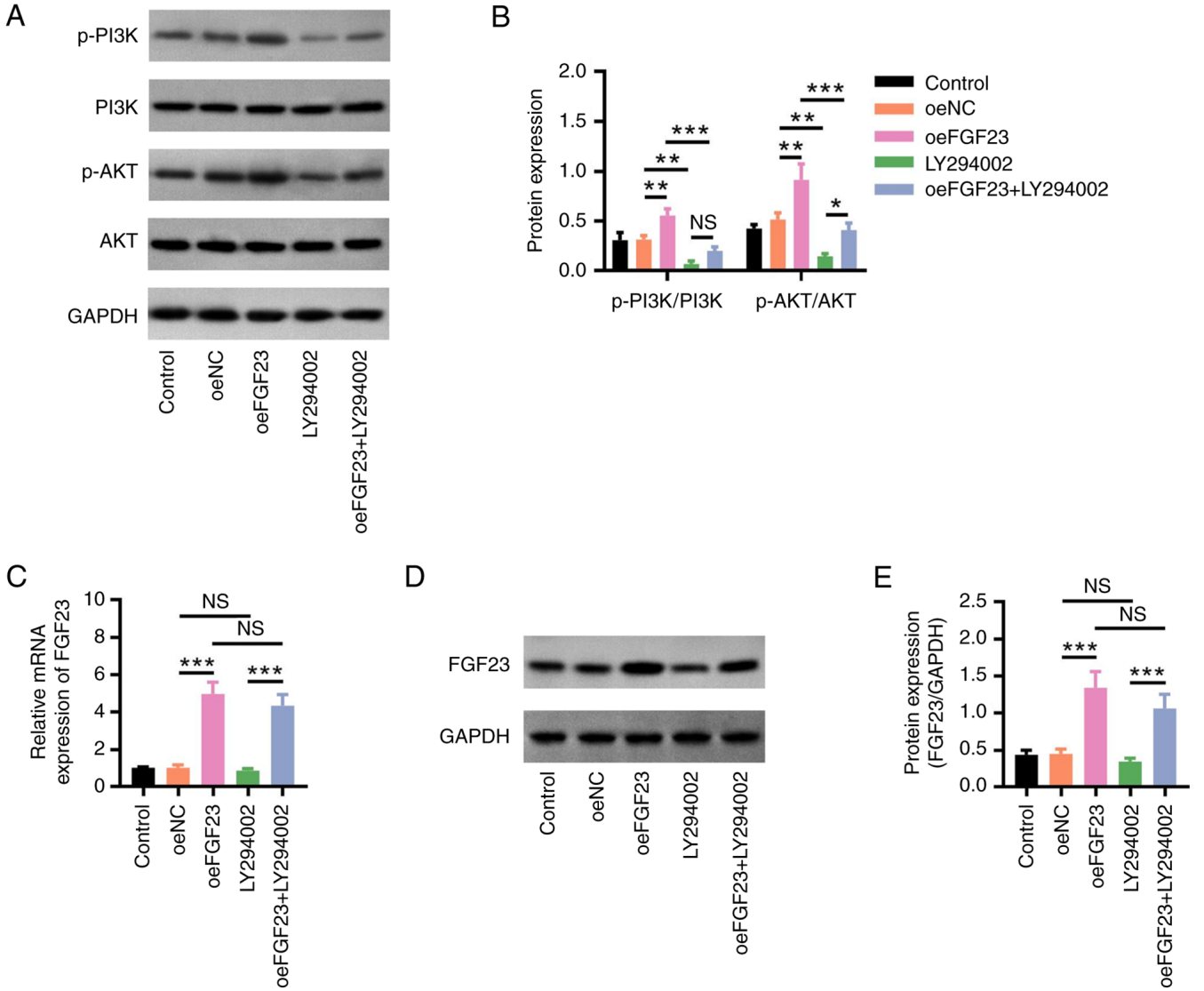

Figure 4. LY294002 reverses the effect of FGF23 on PI3K/AKT signalling. (A) Representative western blotting images and (B) relative protein expression ratios of p-PI3K/PI3K and p-AKT/AKT in the control, oeNC, oeFGF23, LY294002 and oeFGF23 + LY294002 groups. (C) Relative mRNA expression levels of FGF23. (D) Representative western blotting images and (E) relative protein expression levels of FGF23. *P<0.05, **P<0.01 and ***P<0.001. FGF23, fibroblast growth actor 23; NC, negative control; NS, not significant; oe, overexpression; p-, phosphorylated.

accomplished using the H&E staining kit (Wuhan Servicebio Technology Co., Ltd.) according to the manufacturer's instructions. The images were captured using a light microscope (Olympus Corporation). TUNEL staining was performed using a One Step TUNEL Apoptosis Assay Kit (Beyotime Institute of Biotechnology) according to the manufacturer's protocol. The images were observed using an inverted fluorescence microscope (Olympus Corporation).

ELISA. The spinal cord lesion tissues were lysed in RIPA buffer (Beyotime Institute of Biotechnology) and the supernatant was collected by centrifugation (10,000 x g; 15 min; 4˚C). Subsequently, the supernatant was quantified using a BCA kit (Beijing Solarbio Science & Technology Co., Ltd.). Rat TNF-α (cat. no. D731168), IL-1β (cat. no. D731007) and IL-6 (cat. no. D731010) ELISA kits (Sangon Biotech Co., Ltd.) were then used according to the manufacturer's instructions. The absorbance at 450 nm was assessed using a microplate reader (BioTek Instruments, Inc.).

Western blotting. The primary neurons or spinal cord lesion tissues were lysed using RIPA buffer. After quantification using a BCA kit, a total of 50 μg protein/lane was separated by SDS-PAGE on precast 10% gels (Willget) and transferred onto nitrocellulose membranes (Wuhan Servicebio Technology Co., Ltd.). The membranes were then blocked with 5% BSA (Wuhan Servicebio Technology Co., Ltd.) at 37˚C for 1.5 h and incubated overnight at 4˚C with the following primary antibodies: Anti-FGF23 (cat. no. DF3596; 1:500; Affinity Biosciences), anti-cleaved (C)-caspase3 (cat. no. AF7022; 1:1,000; Affinity Biosciences), anti-Bcl-2 (cat. no. AF6139; 1:1,000; Affinity Biosciences), anti-phosphorylated (p)-PI3K (cat. no. ab182651; 1:2,000; Abcam), anti-PI3K (cat. no. ab191606; 1:2,000; Abcam), anti-p-AKT (cat. no. ab38449; 1:2,000; Abcam), anti-AKT (cat. no. ab8805; 1:2,000; Abcam) or anti-GAPDH (cat. no. T0004; 1:4,000; Affinity Biosciences). Following incubation with HRP-conjugated secondary antibodies for 1 h at 37˚C (cat. nos. S0001and S0002; 1:10,000; Affinity Biosciences), the protein bands were visualized using

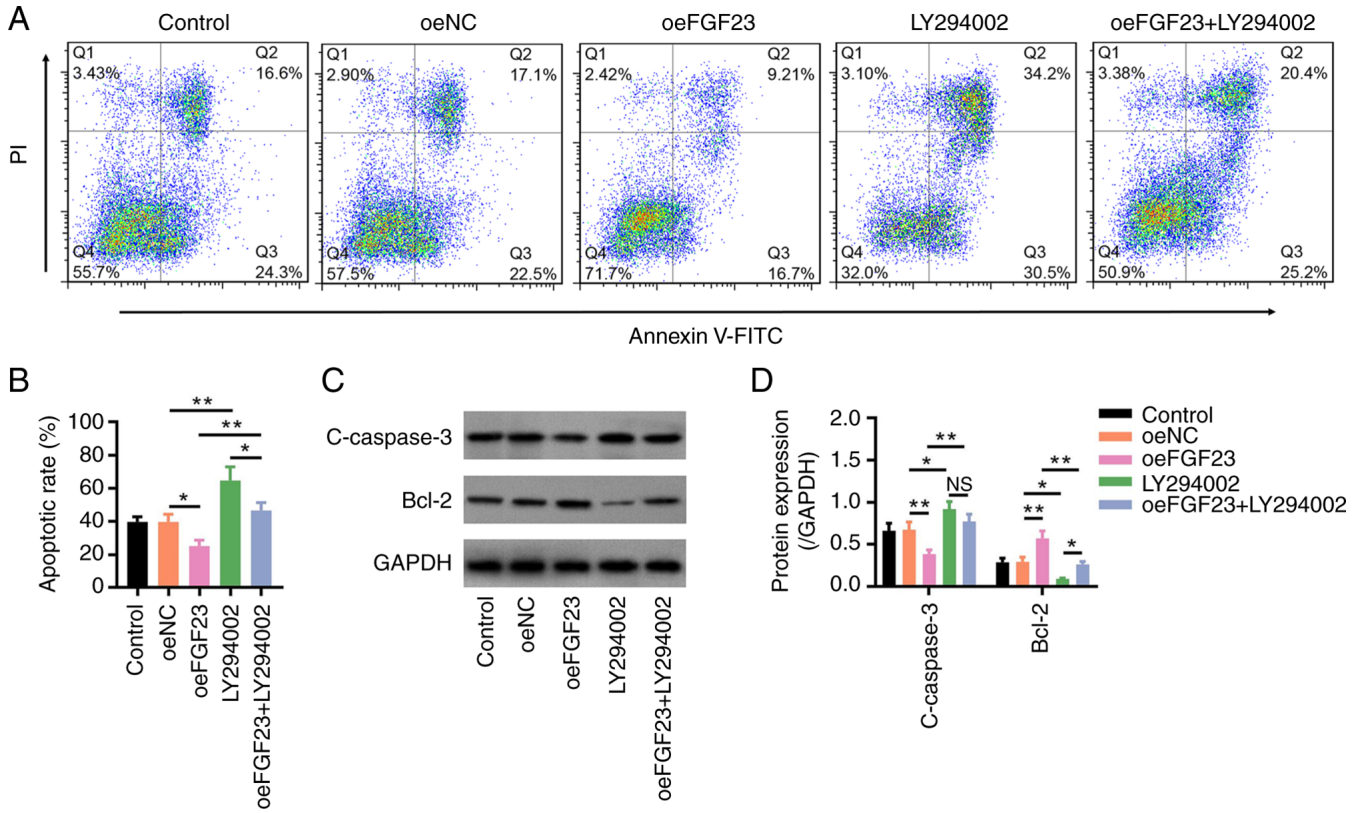

Figure 5. LY294002 reverses the effect of FGF23 on H_2O_2-stimulated neuronal apoptosis. (A) Representative flow cytometry plots of Annexin V/PI staining, and (B) quantification of apoptotic rates in the control, oeNC, oeFGF23, LY294002 and oeFGF23 + LY294002 groups. (C) Representative western blotting images and (D) relative protein expression levels of C-caspase3 and Bcl-2. *P<0.05 and **P<0.01. C-, cleaved; FGF23, fibroblast growth factor 23; NC, negative control; NS, not significant; oe, overexpression.

an Hypersensitive ECL Chemiluminescence Kit (Wuhan Servicebio Technology Co., Ltd.) and semi-quantified using ImageJ software (version 1.52; National Institutes of Health) using GAPDH as the loading control.

Statistical analysis. Quantitative data are presented as the mean ± standard deviation in triplicate and were analysed using GraphPad Prism software (Version 7.0; Dotmatics). Unpaired Student's t-test was used for comparisons between two groups. BBB scoring was analysed using Kruskal-Wallis test with Dunn's post hoc test. For other indexes, one-way ANOVA followed by Tukey's multiple comparisons test was used for comparisons among three or more groups. P<0.05 was considered to indicate a statistically significant difference.

Results

Cell apoptosis, FGF23 and PI3K/AKT signalling in H_2O_2-stimulated primary neurons. Primary neurons were treated with H_2O_2 to establish a cellular model of SCI (17). The results revealed that the apoptotic rate was higher in the H_2O_2 group compared with that in the normal group (P<0.001; Fig. 1A and B). Furthermore, C-caspase3 expression levels were higher (P<0.01), whereas Bcl-2 expression levels were lower (P<0.05) in the H_2O_2 group compared with those in the normal group (Fig. 1C and D). Additionally, the protein (P<0.05; Fig. 1E and F) and mRNA expression levels of FGF23 (P<0.05; Fig. 1G) were decreased in the H_2O_2 group compared with those in the normal group; the protein expression ratios of p-PI3K/PI3K and p-AKT/AKT were both decreased in the H_2O_2 group compared with those in the normal group (both P<0.01; Fig. 1H and I).

Effect of FGF23 on neuronal apoptosis and PI3K/AKT signalling. The mRNA and protein expression levels of FGF23 were higher in the oeFGF23 group compared with those in the oeNC group (both P<0.001), whereas the mRNA and protein expression levels of FGF23 were lower in the shFGF23 group compared with those in the shNC group (both P<0.05) (Fig. 2A-C), which implied successful infection. The apoptotic rate was lower in the oeFGF23 group compared with that in the oeNC group (P<0.01), whereas it was higher in the shFGF23 group compared with that in the shNC group (P<0.05) (Fig. 2D and E). Additionally, the protein expression levels of C-caspase3 were lower in the oeFGF23 group compared with those in the oeNC group and higher in the shFGF23 group compared with those in the shNC group (both P<0.05), whereas Bcl-2 showed the opposite trend (oeFGF23 vs. oeNC, P<0.01; shFGF23 vs. shNC, P<0.05) (Fig. 2F and G).

Regarding PI3K/AKT signalling, the p-PI3K/PI3K (P<0.001) and p-AKT/AKT (P<0.01) protein ratios were higher in the oeFGF23 group compared with those in the oeNC group, whereas the relative protein expression levels of p-PI3K/PI3K (P<0.05) and p-AKT/AKT (P<0.05) were lower in the shFGF23 group compared with those in the shNC group (Fig. 3).

Effects of FGF23 and LY294002 on PI3K/AKT signalling and neuronal apoptosis. The p-PI3K/PI3K and p-AKT/AKT protein ratios were decreased in the LY294002 group compared with those in the oeNC group (both P<0.01); they were also lower in the oeFGF23 + LY294002 group compared with those in the oeFGF23 group, which implied that LY294002 decreased the effect of FGF23 on PI3K/AKT signalling (both P<0.001) (Fig. 4A and B). FGF23 mRNA and protein expression levels did not differ between the LY294002 and oeNC groups nor between the oeFGF23 + LY294002 and oeFGF23 groups, which indicated that LY294002 did not affect FGF23 expression (both P>0.05; Fig. 4C-E).

The apoptotic rate was higher in the LY294002 group compared with that in the oeNC group and this was also increased in the oeFGF23 + LY294002 group compared with that in the oeFGF23 group (both P<0.01; Fig. 5A and B). In addition, the protein expression levels of C-caspase3 were increased, whereas those of Bcl-2 were decreased in the LY294002 group compared with those in the oeNC group (both P<0.05) and in the oeFGF23 + LY294002 group compared with those in the oeFGF23 group (both P<0.01) (Fig. 5C and D). These results indicated that LY294002 reduced the effect of FGF23 on neuronal apoptosis.

Effects of FGF23 and LY294002 on PI3K/AKT signalling, locomotion recovery and inflammation in SCI model rats. FGF23 protein expression was decreased in rats in the SCI model group compared with those in the sham group (P<0.05), whereas it was increased in the SCI + oeFGF23 group compared with that in the SCI + oeNC group (P<0.001) (Fig. 6A and B). Additionally, the protein expression levels of FGF23 did not differ significantly between the SCI + oeFGF23 + LY294002 and SCI + oeFGF23 groups (P>0.05). Furthermore, the p-PI3K/PI3K and p-AKT/AKT protein expression ratios were increased in the SCI + oeFGF23 group compared with those in the SCI + oeNC group (both P<0.05; Fig. 6C and D). The p-PI3K/PI3K (P<0.01) and p-AKT/AKT (P<0.05) ratios were decreased in the SCI + oeFGF23 + LY294002 group compared with those in the SCI + oeFGF23 group, which indicated that LY294002 decreased the effect of FGF23 on PI3K/AKT signalling in SCI model rats.

Moreover, laceration and inflammatory cell infiltration were reduced in the SCI + oeFGF23 group compared with those in the SCI + oeNC group, whereas they increased in the SCI + oeFGF23 + LY294002 group compared with those in the SCI + oeFGF23 group (Fig. 7A). The BBB score (on day 28) was increased in the SCI + oeFGF23 group compared with that in the SCI + oeNC group (P<0.05) but decreased in the SCI + oeFGF23 + LY294002 group compared with that in the SCI + oeFGF23 group (P<0.01) (Fig. 7B). Furthermore, TNF-α (P<0.01; Fig. 7C) and IL-1β (P<0.05; Fig. 7D) levels were lower, whereas IL-6 levels were not altered (P>0.05; Fig. 7E) in the SCI + oeFGF23 group compared with those in the SCI + oeNC group. The TNF-α (P<0.001), IL-1β (P<0.01) and IL-6 (P<0.05) levels were higher in the SCI + oeFGF23 + LY294002 group compared with those in the SCI + oeFGF23 group. Overall, FGF23 overexpression suppressed tissue injury and inflammation, and improved locomotion recovery in rats with SCI, which was reversed by LY294002.

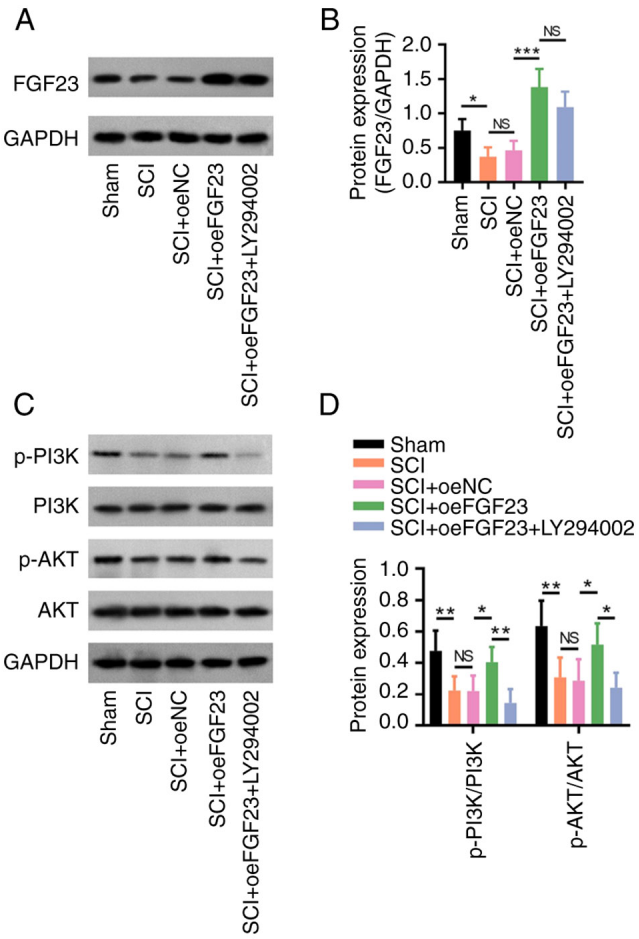

Figure 6. FGF23 activates PI3K/AKT signalling in SCI model rats. (A) Representative western blotting images and (B) relative protein expression levels of FGF23 in the sham, SCI, SCI + oeNC, SCI + oeFGF23 and SCI + oeFGF23 + LY294002 groups. (C) Representative western blotting images and (D) protein expression ratios of p-PI3K/PI3K and p-AKT/AKT. *P<0.05, **P<0.01 and ***P<0.001. FGF23, fibroblast growth factor 23; NC, negative control; NS, not significant; oe, overexpression; p-, phosphorylated; SCI, spinal cord injury.

The number of TUNEL-positive cells was decreased in the SCI + oeFGF23 group compared with that in the SCI + oeNC group (P<0.05); however, the number of TUNEL-positive cells was increased in the SCI + oeFGF23 + LY294002 group compared with that in the SCI + oeFGF23 group (P<0.001; Fig. S1). This finding indicated that FGF23 suppressed apoptosis in rats with SCI, which was reversed by LY294002.

Discussion

The FGF protein family exhibits a protective effect against neural injury. For example, one study reported that FGF2 enhanced the axonal regeneration of human dental pulp cells (25). Another study revealed that FGF1 could prevent motor neuron apoptosis (26). FGF23 may revitalize neural viability through the activation of Na^+/K^+-ATPase (12), which also regulates neural morphology and synaptic growth via the FGF-receptor-mediated AKT pathway (11). However, to the best of our knowledge, the effects of FGF23 on SCI has not yet been reported. The present study revealed that FGF23 reduced the apoptosis of H_2O_2-treated neuronsFGF23 exhibits

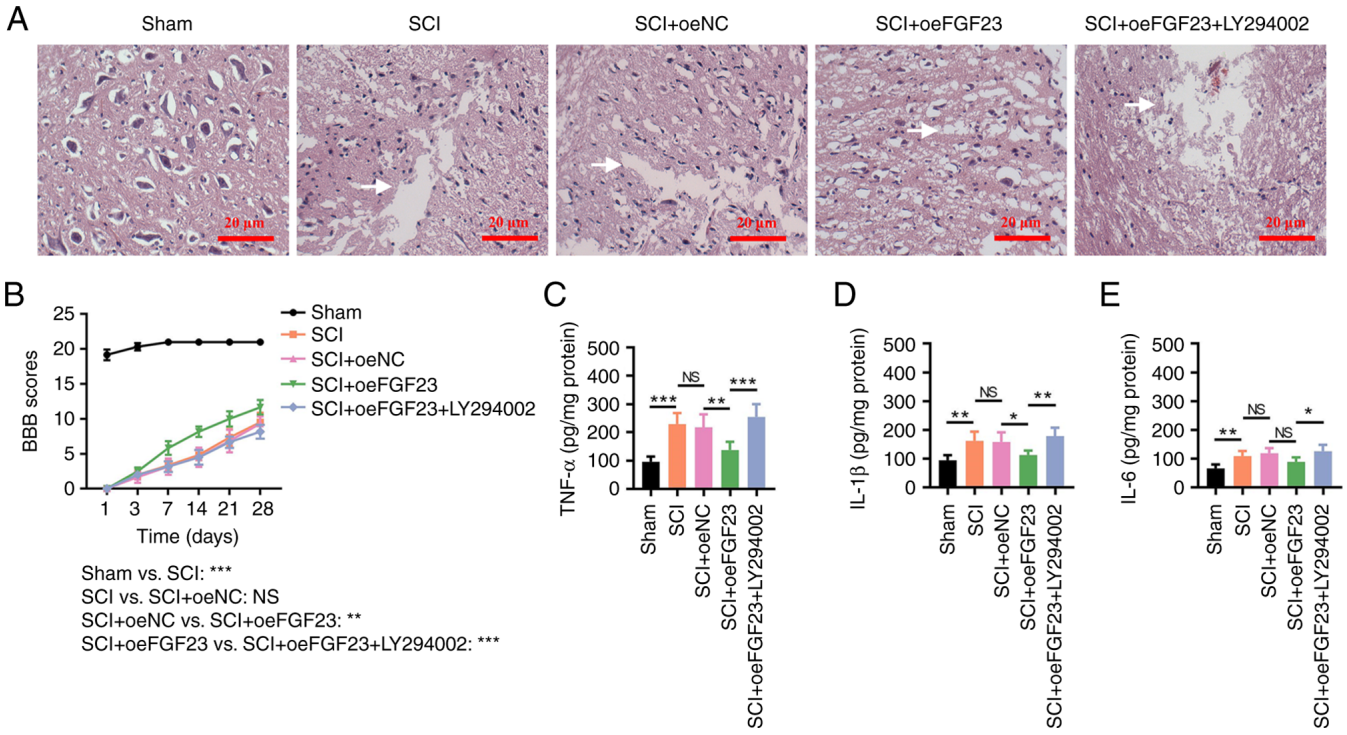

Figure 7. FGF23 improves tissue injury, locomotor function and inflammation in SCI model rats. (A) Histomorphological changes in the sham, SCI, SCI + oeNC, SCI + oeFGF23 and SCI + oeFGF23 + LY294002 groups; the white arrow indicates laceration. (B) BBB scores at 1, 3, 7, 14, 21 and 28 days after surgery;the comparison between groups was carried out on day 28. (C) TNF-α, (D) IL-1β and (E) IL-6 levels. The intercellular space could indicate the presence of a laceration; the larger the intercellular space the more aggravated the laceration. For instance, in Fig. 7A, there is no intercellular space in Sham group, and this means that there is no laceration. However, the intercelluar space is obvious in SCI group, which means that there is laceration. *P<0.05, **P<0.01 and ***P<0.001. BBB, Basso-Beattie-Bresnahan; FGF23, fibroblast growth factor 23; NC, negative control; NS, not significant; oe, overexpression; SCI, spinal cord injury.

a protective role in primary neurons, and it may inhibit the apoptosis of neurons through activating the PI3K/AKT signalling (11,12,27,28). It should be noted that in the present study, inflammatory cytokines were only detected *in vivo* but not *in vitro*; the reason for this issue was that the primary neurons used in the *in vitro* study were collected from the cerebral cortex of the foetal rat, which did not secrete inflammatory cytokines (29). Hence, the levels of inflammatory cytokines were not measured in the present *in vitro* study.

PI3K/AKT signalling activation has been confirmed to have a protective role in SCI. For example, one study reported that the PI3K/AKT signalling pathway can suppress neurotoxic microglia and astrocytes to improve SCI recovery (30), and another study revealed that the PI3K/AKT pathway can attenuate neural pyroptosis during SCI (31). In addition, it has been reported that FGF23 may be a stimulator of PI3K/AKT signalling (28,32,33). A previous study revealed that FGF23 could interact with PI3K/AKT signalling in diabetic mice (32). Additionally, another study reported that FGF23 induced the activation of PI3K/AKT signalling in transgenic α-Klotho mice (28). Additionally, FGF23 can modulate PI3K/AKT signalling in osteoblasts (33). In terms of neuron regulation, a previous study showed that FGF23 increased the activity of hippocampal cells via stimulation of PI3K/AKT signalling (11). Based on the aforementioned body of evidence, PI3K/AKT regulation experiments were further performed in the current study, which demonstrated that FGF23 exhibited a protective effect on apoptosis via upregulation of PI3K/AKT signalling in H_2O_2-treated neurons, which was partly in agreement with previous findings (11,28,33). However, the underlying mechanism of the regulatory role of FGF23 in PI3K/AKT signalling still requires further investigation.

In addition to the aforementioned findings, results from the present study further demonstrated that FGF23 decreased neuroinflammation via activation of PI3K/AKT signalling in SCI model rats. The possible explanations are as follows: i) FGF23 maintains the property of neurons in SCI model rats, further promoting the formation of glia limitans, which might help to restrict the recruitment of inflammatory factors; thus, FGF23 decreases inflammation in SCI model rats (34,35); and ii) PI3K/AKT inhibits gasdermin D-mediated microglia pyroptosis directly to suppress inflammation (31). Additionally, the present study investigated the effect of FGF23 on locomotion recovery in a rat model of SCI and revealed that FGF23 improved the locomotion recovery in a PI3K/AKT-dependent manner, which might improve neural inflammation and apoptosis. Furthermore, the effect of LY294002 on SCI and its compensation effect on FGF23 was assessed *in vitro*; however, the effect of LY294002 monotherapy on SCI rats was not assessed *in vivo*. The reason for this was that the effect of LY294002 in SCI model rats had already been assessed in the previous studies (19,22), hence, the current study did not re-assess this documented issue.

In conclusion, FGF23 alleviated neuronal apoptosis and inflammation, and it promoted locomotion recovery via

activation of PI3K/AKT signalling in SCI, indicating its potential as a treatment option for SCI; however, further studies are warranted for validation.

Acknowledgements

Not applicable.

Funding

No funding was received.

Availability of data and materials

The datasets used and/or analysed during the current study are available from the corresponding author on reasonable request.

Authors' contributions

ZL and WF substantially contributed to the conception and design of the study. YC and BY were responsible for the acquisition of the data. SL and LH contributed to the data analysis. FX contributed to the interpretation of data. ZL, WF and YC confirm the authenticity of all the raw data. All authors read and approved the final manuscript.

Ethics approval and consent to participate

All procedures followed in the present study were approved by the Animal Care and Use Committee of Xiamen University (approval no. 20210401).

Patient consent for publication

Not applicable.

Competing interests

The authors declare that they have no competing interests.

References

1. Hachem LD and Fehlings MG: Pathophysiology of spinal cord injury. Neurosurg Clin N Am 32: 305-313, 2021.
2. Lee BJ and Jeong JH: Review: Steroid use in patients with acute spinal cord injury and guideline update. Korean J Neurotrauma 18: 22-30, 2022.
3. Anjum A, Yazid MD, Fauzi Daud M, Idris J, Ng AMH, Selvi Naicker A, Ismail OHR, Athi Kumar RK and Lokanathan Y: Spinal cord injury: Pathophysiology, multimolecular interactions, and underlying recovery mechanisms. Int J Mol Sci 21: 7533, 2020.
4. Eli I, Lerner DP and Ghogawala Z: Acute traumatic spinal cord injury. Neurol Clin 39: 471-488, 2021.
5. Karsy M and Hawryluk G: Modern medical management of spinal cord injury. Curr Neurol Neurosci Rep 19: 65, 2019.
6. Huang H, Young W, Skaper S, Chen L, Moviglia G, Saberi H, Al-Zoubi Z, Sharma HS, Muresanu D, Sharma A, *et al*: Clinical neurorestorative therapeutic guidelines for spinal cord injury (IANR/CANR version 2019). J Orthop Translat 20: 14-24, 2019.
7. Patsakos EM, Bayley MT, Kua A, Cheng C, Eng J, Ho C, Noonan VK, Querée M and Craven BC; Can-SCIP Guideline Expert Panel: Development of the Canadian spinal cord injury best practice (Can-SCIP) guideline: Methods and overview. J Spinal Cord Med 44 (Suppl 1): S52-S68, 2021.
8. Alam R, Mrad Y, Hammoud H, Saker Z, Fares Y, Estephan E, Bahmad HF, Harati H and Nabha S: New insights into the role of fibroblast growth factors in Alzheimer's disease. Mol Biol Rep 49: 1413-1427, 2022.
9. Klimaschewski L and Claus P: Fibroblast growth factor signalling in the diseased nervous system. Mol Neurobiol 58: 3884-3902, 2021.
10. Vervloet MG: Shedding light on the complex regulation of FGF23. Metabolites 12: 401, 2022.
11. Hensel N, Schön A, Konen T, Lübben V, Förthmann B, Baron O, Grothe C, Leifheit-Nestler M, Claus P and Haffner D: Fibroblast growth factor 23 signaling in hippocampal cells: Impact on neuronal morphology and synaptic density. J Neurochem 137: 756-769, 2016.
12. Oshima N, Onimaru H, Yamagata A, Ito S, Imakiire T and Kumagai H: Rostral ventrolateral medulla neuron activity is suppressed by Klotho and stimulated by FGF23 in newborn Wistar rats. Auton Neurosci 224: 102640, 2020.
13. Musgrove J and Wolf M: Regulation and effects of FGF23 in chronic kidney disease. Annu Rev Physiol 82: 365-390, 2020.
14. Zhang X, Guo K, Xia F, Zhao X, Huang Z and Niu J: $FGF23^{C\text{-}tail}$ improves diabetic nephropathy by attenuating renal fibrosis and inflammation. BMC Biotechnol 18: 33, 2018.
15. Guidelines for Endpoints in Animal Study Proposals. Available at: https://oacu.oir.nih.gov/system/files/media/file/2022-04/b13_endpoints_guidelines.pdf.
16. Yang H, Wang H, Shu Y and Li X: miR-103 promotes neurite outgrowth and suppresses cells apoptosis by targeting prostaglandin-endoperoxide synthase 2 in cellular models of Alzheimer's disease. Front Cell Neurosci 12: 91, 2018.
17. Wang N, Yang Y, Pang M, Du C, Chen Y, Li S, Tian Z, Feng F, Wang Y, Chen Z, *et al*: MicroRNA-135a-5p promotes the functional recovery of spinal cord injury by targeting SP1 and ROCK. Mol Ther Nucleic Acids 22: 1063-1077, 2020.
18. Luo Z, Wu F, Xue E, Huang L, Yan P, Pan X and Zhou Y: Hypoxia preconditioning promotes bone marrow mesenchymal stem cells survival by inducing HIF-1α in injured neuronal cells derived exosomes culture system. Cell Death Dis 10: 134, 2019.
19. Zhao R, Wu X, Bi XY, Yang H and Zhang Q: Baicalin attenuates blood-spinal cord barrier disruption and apoptosis through PI3K/Akt signaling pathway after spinal cord injury. Neural Regen Res 17: 1080-1087, 2022.
20. Livak KJ and Schmittgen TD: Analysis of relative gene expression data using real-time quantitative PCR and the 2(-Delta Delta C(T)) method. Methods 25: 402-408, 2001.
21. Li X, Zhang C, Haggerty AE, Yan J, Lan M, Seu M, Yang M, Marlow MM, Maldonado-Lasunción I, Cho B, *et al*: The effect of a nanofiber-hydrogel composite on neural tissue repair and regeneration in the contused spinal cord. Biomaterials 245: 119978, 2020.
22. Chen J, Wang Z, Zheng Z, Chen Y, Khor S, Shi K, He Z, Wang Q, Zhao Y, Zhang H, *et al*: Neuron and microglia/macrophage-derived FGF10 activate neuronal FGFR2/PI3K/Akt signaling and inhibit microglia/macrophages TLR4/NF-κB-dependent neuroinflammation to improve functional recovery after spinal cord injury. Cell Death Dis 8: e3090, 2017.
23. Wang H, Zheng Z, Han W, Yuan Y, Li Y, Zhou K, Wang Q, Xie L, Xu K, Zhang H, *et al*: Metformin promotes axon regeneration after spinal cord injury through inhibiting oxidative stress and stabilizing microtubule. Oxid Med Cell Longev 2020: 9741369, 2020.
24. AVMA Guidelines for the Euthanasia of Animals: 2020 Edition. Available at: https://olaw.nih.gov/avma-guidelines-2020.htm.
25. Nagashima K, Miwa T, Soumiya H, Ushiro D, Takeda-Kawaguchi T, Tamaoki N, Ishiguro S, Sato Y, Miyamoto K, Ohno T, *et al*: Priming with FGF2 stimulates human dental pulp cells to promote axonal regeneration and locomotor function recovery after spinal cord injury. Sci Rep 7: 13500, 2017.
26. Vargas MR, Pehar M, Cassina P, Martínez-Palma L, Thompson JA, Beckman JS and Barbeito L: Fibroblast growth factor-1 induces heme oxygenase-1 via nuclear factor erythroid 2-related factor 2 (Nrf2) in spinal cord astrocytes: Consequences for motor neuron survival. J Biol Chem 280: 25571-25579, 2005.
27. Kma L and Baruah TJ: The interplay of ROS and the PI3K/Akt pathway in autophagy regulation. Biotechnol Appl Biochem 69: 248-264, 2022.
28. Xiao Z, King G, Mancarella S, Munkhsaikhan U, Cao L, Cai C and Quarles LD: FGF23 expression is stimulated in transgenic alpha-Klotho longevity mouse model. JCI Insight 4: e132820, 2019.

29. Mills S: Histology for Pathologists (5th edition). Wolters Kluwer health, chapter 9, pp224-232, 2019.
30. Jiang D, Gong F, Ge X, Lv C, Huang C, Feng S, Zhou Z, Rong Y, Wang J, Ji C, *et al*: Neuron-derived exosomes-transmitted miR-124-3p protect traumatically injured spinal cord by suppressing the activation of neurotoxic microglia and astrocytes. J Nanobiotechnology 18: 105, 2020.
31. Xu S, Wang J, Zhong J, Shao M, Jiang J, Song J, Zhu W, Zhang F, Xu H, Xu G, *et al*: CD73 alleviates GSDMD-mediated microglia pyroptosis in spinal cord injury through PI3K/AKT/Foxo1 signaling. Clin Transl Med 11: e269, 2021.
32. Luo W, Jiang Y, Yi Z, Wu Y, Gong P and Xiong Y: 1a,25-Dihydroxyvitamin D_3 promotes osteogenesis by down-regulating FGF23 in diabetic mice. J Cell Mol Med 25: 4148-4156, 2021.
33. Xiao Z, Huang J, Cao L, Liang Y, Han X and Quarles LD: Osteocyte-specific deletion of Fgfr1 suppresses FGF23. PLoS One 9: e104154, 2014.
34. O'Shea TM, Burda JE and Sofroniew MV: Cell biology of spinal cord injury and repair. J Clin Invest 127: 3259-3270, 2017.
35. Hellenbrand DJ, Quinn CM, Piper ZJ, Morehouse CN, Fixel JA and Hanna AS: Inflammation after spinal cord injury: A review of the critical timeline of signaling cues and cellular infiltration. J Neuroinflammation 18: 284, 2021.